AIMS Mathematics, 7(7): 13053–13073.
DOI: 10.3934/math.2022722
Received: 21 February 2022
Revised: 13 April 2022
Accepted: 19 April 2022
Published: 09 May 2022

http://www.aimspress.com/journal/Math

*Research article*

# Mathematical modeling and analysis of the effect of the rugose spiraling whitefly on coconut trees

**Suganya Govindaraj and Senthamarai Rathinam***

Department of Mathematics, College of Engineering and Technology, SRM Institute of Science and Technology, Kattankulathur-603203, Tamilnadu, India

* **Correspondence:** Email: senthamr@srmist.edu.in.

**Abstract:** Coconut trees are severely affected by the rugose spiraling whitefly (Aleurodicus rugioperculatus Martin), which is an exotic pest. The dynamics of the disease caused by this pest are analyzed using a mathematical model. The equilibrium points are proved to be locally and globally asymptotically stable under some conditions. Our study, with sensitivity analysis, reveals that the contact rate plays a crucial role in the system that has a direct impact on disease spread. Further, with optimal control, we evoke the optimum level of spraying insecticide, which results in better control over disease with minimum cost of spraying. Additionally, an approximate analytical solution has been derived using a homotopy analysis method. The $\hbar$-curves are provided to validate the region of convergence. The analytical results are compared with the results of numerical simulation and they are found to be in good agreement. Our goal is to keep the spread under control so that yield is unaffected. Controlling the contact rate with control measures can reduce the risk of healthy trees becoming infected and the intensity of infection.

**Keywords:** mathematical model; coconut trees; rugose spiraling whitefly; stability; analytical approximation; sensitivity analysis; optimal control
**Mathematics Subject Classification:** 34D20, 37N25, 92-10, 92D25, 92D45

## 1. Introduction

The coconut tree (Cocos nucifera) belongs to the palm tree family and is the only living species of the genus Cocos. The coconut tree deserves to be one of the most useful trees, hence the name “tree of life”. Coconut is especially known for its diverse usage, ranging from health benefits to building materials. Coconuts are very distinct from other fruits because of the effective usage of each and every constituent. Over 93 countries in the world have coconut plantations with a plantation area of about 12 million hectares, leading to an annual nut production of 59.98 million tonnes. Indonesia leads

the list with an annual production of 18 million tonnes. The Philippines stands second with 15.86 million tonnes. India holds the third position with 10.56 million tons of coconuts. The major coconut-producing states in India are Kerala, Karnataka, Tamil Nadu, Orissa, Maharashtra, West Bengal and Assam. India consumes around 50% of its annual production. Numerous pests pose various risks in bringing up these coconut trees. The rugose spiraling whitefly (RSW), an invasive whitefly species belonging to the Aleyrodidae family, originally called a gumbo limbo spiraling whitefly, was first reported in coconut in 2004 in Belize, Central America [1]. The RSW is an exotic pest affecting coconut trees since 2016 in India. The pest was reported for the first time on coconut trees in Pollachi, Tamil Nadu in India during August 2016 [2–4]. This pest was soon reported on various other plants such as mango, guava, sapota, custard apple and banana plants, as well as on many other economically important ornamental plants. The RSW invasion will pose high risk to the coconut industry in India by reducing the overall production rate and quality of the flesh produced and increasing the production cost for the management of pests [5]. This whitefly affects the host tree since its feeding removes both the nutrients and water content from the leaves. Further, it leaves sooty mold, which covers the leaf surface and potentially reduces the photosynthesis process, thereby affecting the yield and growth [6].

The formulation and concept of mathematical models in epidemiology have been explained [7]. The role of mathematical models explains the dynamics of the interacting population. These models help to understand the impact and interactions between the variables and parameters and provide biological interpretation. In obtaining high yield and healthy crops in agriculture, pest control plays a significant role. The dynamics of plant and vector populations within a locality have been studied for African cassava mosaic virus disease (ACMD). An unexploited class of model that links vector dynamics and virus epidemiology for ACMD has been developed in a system of differential equations [8]. The impact of incubation delay in plant-vector interaction has been studied [9]. A mathematical model has been formulated in order to examine the effect of farming awareness in controlling the pest [10]. In literature, many models have been developed to reduce the effect of mosaic disease in Jatropha Curcas plantations. These models incorporate the impact of awareness, roguing and pest control to examine its dynamics [10–12]. A generalized delay-induced epidemic model with a nonlinear incidence rate, latency and relapse has been studied [13]. A mathematical study using an SIR model with a convex incidence rate has been carried out [14]. In any infectious disease, the main concern lies in the ability of the disease to invade a population. The epidemiological models usually have a threshold parameter called the basic reproduction number, which can identify whether the disease could invade the population. The models use the next-generation matrix to examine the reproduction number [15]. The stability of dynamical systems based on extensions of Lyapunov's direct method have been presented for difference and differential equations [16].

In mathematical models related to biological or physical phenomena, the characterization of the connection between the observed solution and parameters of the system is desirable. This type of analysis is called sensitivity analysis. The values obtained from the analysis specify the state variable in the direction of a chosen parameter at a time $t$ [17, 18]. The term integrated control means the combination of biological methods and chemical control methods. The dynamics of the model with fixed control has been investigated using MATLAB [19–21].

There are several methods to solve this kind of nonlinear problem. Analytical methods like the variational iteration method, Adomian decomposition method, homotopy perturbation methods and some other methods are applicable to provide approximate solutions for nonlinear differential

equations [22–24]. Liao proposed an analytical method to solve the nonlinear problems by overcoming the restrictions of perturbation techniques [25, 26]. This method has the advantage that we can control and adjust the rate of the approximation series and convergence region by allowing an auxiliary parameter $\hbar$ to vary [27–30]. It gives an exact solution even if the nonlinear problem does not possess small or large parameters. By selecting alternative sets of base functions, it can be used to efficiently approximate a nonlinear problem. Recently, a number of mathematical studies and structures have been carried out on plant epidemics. The infection dynamics for a butterfly pathogen, mosaic disease with microbial biostimulants and huanglongbing transmission within a citrus tree has been analyzed [31–34]. A fractional mathematical model for stimulating the dynamics of fungicide application has been derived and analyzed [35].

To the best of our knowledge, there is no differential equation system that models RSWs affecting coconut trees. Motivated by the plant-vector interaction model [9], we analyzed the dynamics of the disease using a mathematical model. We mainly focus on the Pollachi tract in Tamil Nadu, and the parameter values are considered based on it. We observed its stability at the equilibrium points. The reproduction number was obtained using a next-generation matrix. For the sensitivity analysis, we studied the parameters affecting the system. Then, an optimal control problem was formulated and optimal control was achieved using the Pontryagin minimum principle. Also, we obtained an approximate analytical solution using a homotopy analysis method (HAM).

## 2. Mathematical formulation

A plant-vector interaction model [9] without delay was developed by considering the coconut trees and whitefly population to examine the impact of RSWs on coconut trees. The tree population was divided into healthy and infected trees, denoted by $H$ and $I$, respectively. $W$ denotes the whitefly population. We have considered the population density per square meter as in [8]. The mathematical model is proposed as follows:

$$\frac{dH}{dt} = rH\left(1 - \frac{H+I}{k}\right) - \alpha HW, \tag{2.1}$$

$$\frac{dI}{dt} = \alpha HW - pI, \tag{2.2}$$

$$\frac{dW}{dt} = qI - \zeta W, \tag{2.3}$$

with the following initial conditions:

$$H(0) = H_0, \;\; I(0) = I_0, \;\; W(0) = W_0. \tag{2.4}$$

We assume that $H_0 > 0$, $I_0 > 0$ and $W_0 > 0$. The healthy trees follow logistic growth with the tree density $k$ measured as density per square meter. Let $\alpha$ be the contact rate between RSWs and healthy trees, with the unit of pest$^{-1}$day$^{-1}$. Let $p$ be the mortality rate for infected trees, $r$ denote the replanting rate, $q$ denote the birth rate for RSWs and $\zeta$ be its mortality rate; the rates are measured as day$^{-1}$.

## 3. Mathematical analysis of the model

### 3.1. Positivity and boundedness

From the system described by Eqs (2.1)–(2.4), we see that

$$\left.\frac{dH}{dt}\right|_{H=0,I>0,W>0} = 0,\ \left.\frac{dI}{dt}\right|_{H>0,I=0,W>0} = \alpha HW \geq 0,\ \left.\frac{dW}{dt}\right|_{H>0,I>0,W=0} = qI \geq 0. \tag{3.1}$$

Hence, the solution exists in the region $\mathbb{R}^3_+$, and the solution is positive for some sufficiently small $t > 0$.

The total tree population $N = H + I$ satisfies

$$\frac{dH}{dt} + \frac{dI}{dt} = rH\left(1 - \frac{H+I}{k}\right) - \alpha HW + \alpha HW - pI,$$

$$\frac{d(H+I)}{dt} + \eta H + \eta I = rH\left(1 - \frac{H+I}{k}\right) - pI + \eta H + \eta I,$$

$$\frac{dN}{dt} + \eta N \leq -rH\left(\frac{N}{k}\right) + (r+\eta)H + (\eta - p)I,$$

$$\frac{dN}{dt} + \eta N \leq -\frac{rH^2}{k} + (r+\eta)H,$$

Here $\eta < p$. It is seen that $-\frac{rH^2}{k} + (r+\eta)H$ is quadratic in $H$ and its maximum value is $\frac{(r+\eta)^2 k}{4r}$.

$$\frac{dN}{dt} + \eta N \leq l,$$

where $l = \frac{(r+\eta)^2 k}{4r}$.

$$0 \leq N(t) \leq e^{-\eta t}\left(N(0) - \frac{l}{\eta}\right) + \frac{l}{\eta}. \tag{3.2}$$

As $t \to \infty$, $N(t) \to \frac{l}{\eta}$ since $\sup_{t\to\infty} N(t) = \frac{l}{\eta}$.

Further, $\frac{dW}{dt} = qI - \zeta W$ implies $\sup_{t\to\infty} W(t) = \frac{l}{q\eta}$ as a result of using the bound of $I$.

Thus, the biologically feasible region of the system described by Eqs (2.1)–(2.3) is the following positive invariant set:

$$\Omega = \left\{(H, I, W) \in \mathbb{R}^3_+ \mid 0 \leq H, I \leq \frac{l}{\eta}, W \leq \frac{l}{q\eta}\right\}.$$

### 3.2. Existence of equilibria

The system given by Eqs (2.1)–(2.3) possess three equilibrium points. They are as follows:

- Trivial equilibrium: $E_0 = (0, 0, 0)$
- Pest-free equilibrium: $E_1 = (k, 0, 0)$
- Coexistence equilibrium: $E_* = (H^*, I^*, W^*)$

$$where\ H^* = \frac{p\zeta}{\alpha q},\ I^* = \frac{\zeta r(\alpha kq - p\zeta)}{\alpha q(\zeta r + \alpha kq)},\ W^* = \frac{r(\alpha kq - p\zeta)}{\alpha(\zeta r + \alpha kq)}.$$

### 3.3. Reproduction number

At disease-free equilibrium, we consider the matrices that represent transfer and new infection. The reproduction number is derived using the next-generation matrix [15].

$$R_0 = \frac{\alpha k q}{p\zeta}.$$

### 3.4. Stability analysis

The qualitative behavior of dynamical systems can be studied using local stability analysis. In this section, we implement the stability analysis for the model given by Eqs (2.1)–(2.3).

The Jacobian matrix of the system is given by

$$J(E) = \begin{bmatrix} r\left(1 - \frac{H+I}{k}\right) - \frac{rH}{k} - \alpha W & -\frac{rH}{k} & -\alpha H \\ \alpha W & -p & \alpha H \\ 0 & q & -\zeta \end{bmatrix}.$$

**Lemma:** The system given by Eqs (2.1)–(2.3) around $E_0 = (0, 0, 0)$ is always unstable.

**Theorem 1.** The system given by Eqs (2.1)–(2.3) around the pest-free equilibrium $E_1 = (k, 0, 0)$ is locally asymptotically stable (LAS), provided $R_0 < 1$.

*Proof.* At $E_1$, the Jacobian matrix of the system is given by

$$J(E_1) = \begin{bmatrix} -r & -r & -\alpha k \\ 0 & -p & \alpha k \\ 0 & q & -\zeta \end{bmatrix}.$$

The characteristic equation of the matrix is

$$(-r - \lambda)[(-p - \lambda)(-\zeta - \lambda) - \alpha q k] = 0,$$

which implies

$$\lambda^3 + \lambda^2(r + p + \zeta) + \lambda(rp + r\zeta + p\zeta + \alpha q k) + rp\zeta - r\alpha q k = 0, \tag{3.3}$$

which is of the form $\lambda^3 + \upsilon_1\lambda^2 + \upsilon_2\lambda + \upsilon_3 = 0$.

By the Routh-Hurwitz (R-H) criterion, the system is LAS if $\upsilon_1 > 0$, $\upsilon_3 > 0$ and $\upsilon_1\upsilon_2 > \upsilon_3$. Hence, $E_1$ is LAS if $\alpha q k < p\zeta$, i.e., $R_0 < 1$.

**Theorem 2.** When $R_0 > 1$, the system given by Eqs (2.1)–(2.3) at the coexistence equilibrium $E_* = (H^*, I^*, W^*)$ is LAS if $Q_1 > 0$, $Q_3 > 0$ and $Q_1Q_2 > Q_3$, i.e., $\frac{\alpha k q}{p\zeta} > 1$ and $\frac{\alpha k q - p\zeta}{\zeta r + \alpha k q} > 1$. The terms $Q_1$, $Q_2$ and $Q_3$ are defined in the proof.

*Proof.* The Jacobian matrix of the system at $E_*$ is given by

$$J(E_*) = \begin{bmatrix} r\left(1 - \frac{H^*+I^*}{k}\right) - \frac{rH^*}{k} - \alpha W^* & \frac{-rH^*}{k} & -\alpha H^* \\ \alpha W^* & -p & \alpha H^* \\ 0 & q & -\zeta \end{bmatrix}.$$

The matrix $J(E_*)$ gives the characteristic equation after substituting the equilibrium points as

$$\lambda^3 + Q_1\lambda^2 + Q_2\lambda + Q_3 = 0,$$

where

$$Q_1 = \frac{2rp\zeta}{\alpha qk} + \frac{r(\alpha kq - p\zeta)}{\zeta r + \alpha kq} + p + \zeta - r + \frac{r^2\zeta(\alpha kq - p\zeta)}{\alpha k^2 q(\zeta r + \alpha kq)}, \tag{3.4}$$

$$Q_2 = \frac{2rp\zeta(p+\zeta)}{k\alpha q} + \frac{r^2 p\zeta}{k\alpha q - p\zeta}\left(\frac{\alpha kq}{\zeta r + \alpha kq}\right) + r(p+\zeta)\left(\frac{\alpha kq - p\zeta}{\zeta r + \alpha kq}\right) - r(p+\zeta) + \frac{r^2\zeta(p+\zeta)}{k\alpha q}\left(\frac{\alpha kq - p\zeta}{\zeta r + \alpha kq}\right), \tag{3.5}$$

$$Q_3 = \left(\frac{\alpha kq - p\zeta}{\zeta r + \alpha kq}\right)\left(\frac{r^2 p\zeta^2}{\alpha kq} + rp\zeta\right). \tag{3.6}$$

The roots of the characteristic equation will have negative real parts when $Q_1 > 0$, $Q_3 > 0$ and $Q_1Q_2 > Q_3$. Thus, by R-H criterion, the condition to be LAS is $\frac{\alpha kq}{p\zeta} > 1$ and $\frac{\alpha kq - p\zeta}{\zeta r + \alpha kq} > 1$. Hence, the system given by Eqs (2.1)–(2.3) around $E_*$ is LAS.

**Theorem 3.** The system given by Eqs (2.1)–(2.3) around the pest-free equilibrium $E_1 = (k, 0, 0)$ is globally asymptotically stable (GAS) in $\Omega$ if $R_0 < 1$.

*Proof.* We construct a Lyapunov function $V(H, I, W)$ in $\Omega$ as

$$V(H, I, W) = \frac{m_1}{2}I^2. \tag{3.7}$$

The time derivative of $V$ is computed along the solution of the system as

$$\frac{dV}{dt} = m_1 I\frac{dI}{dt},$$

where $m_1$ is the positive constant.

$$\frac{dV}{dt} = m_1 I[\alpha HI - pI],$$

$$\frac{dV}{dt} = m_1 I^2[R_0 - 1]\frac{\zeta}{q},$$

After choosing $m_1 = \frac{q}{\zeta}$, we get

$$\frac{dV}{dt} = I^2[R_0 - 1] \leq 0.$$

In our model, since all of the parameters are positive and the variables are non-negative, it follows that $\frac{dV}{dt} < 0$ for $R_0 < 1$, with $\frac{dV}{dt} = 0$ if and only if, $I = 0$. Using the Lyapunov and LaSalle theorems [16], we conclude that $E_1$ is GAS.

**Theorem 4.** The coexistence equilibrium $E_*$, whenever it exists, is GAS if the following inequality holds:

$$k < (I + H + H^*),$$
$$m_2 q^2 < 2\zeta\left(p + \frac{rI}{k}\right).$$

*Proof.* We construct a Lyapunov function $V_*(H, I, W)$ in $\Omega$ as

$$V_*(H, I, W) = \frac{1}{2}(H - H^* + I - I^*) + \frac{m_2}{2}(W - W^*)^2, \tag{3.8}$$

$$\frac{dV_*}{dt} = (H - H^* + I - I^*)\left(\frac{dH}{dt} + \frac{dI}{dt}\right) + m_2(W - W^*)\frac{dW}{dt},$$

where $m_2$ is the positive constant. The time derivative of $V_*$ is computed along the solution of the system and, after rearranging the terms, we get

$$\begin{aligned}\frac{dV_*}{dt} = -\left(\frac{r}{k}(I + H + H^*) - r\right)(H - H^*)^2 - \left(\frac{r}{k}(2H^* + H + I^*) - r + p\right)(H - H^*)(I - I^*)\\ -\left(p + \frac{rI}{k}\right)(I - I^*)^2 - m_2\zeta(W - W^*)^2 + m_2q(W - W^*)(I - I^*).\end{aligned}$$

Thus, $\frac{dV^*}{dt}$ will be negative-definite inside the region of attraction provided the following inequalities are satisfied:

$$\begin{aligned}k < (I + H + H^*),\\ m_2q^2 < 2\zeta\left(p + \frac{rI}{k}\right).\end{aligned}$$

It is seen that $\frac{dV_*}{dt} < 0$ and $\frac{dV_*}{dt} = 0$ if, and only if, $H = H^*$, $I = I^*$ *and* $W = W^*$ in $\Omega$. From this inequality, the positive value of $m_2$ may be chosen provided the inequality is satisfied. Using the Lyapunov and LaSalle theorems [16], we conclude that $E_*$ is GAS whenever $R_0 > 1$.

## 4. Sensitivity analysis

Sensitivity analysis helps to evaluate the sensitive parameters of the system. We used MATLAB to perform this analysis. This task formulates differential equations by differentiating the original equations with respect to parameters to calculate the sensitivities. The sensitivity parameters were chosen as $\alpha$, $q$ and $\zeta$ to perform the analysis. Figure 7 denotes the state variables in the direction of the parameters, ie., the partial derivative of the state variables with respect to the selected parameters. It is observed that the contact rate $\alpha$ reduces the healthy tree density and increases the infected tree density. Furthermore, it is to be noted that the death rate for RSWs is able to slightly increase the healthy tree density, slightly decrease infected plant density and reduce the whitefly population. Figure 8 describes the logarithmic sensitivity analysis. The logarithmic sensitivity analysis is the ratio of the relative change in the variable to the relative change in the parameter, ie., the normalized forward sensitivity index of a variable $X$ that depends differentiably on a parameter $a$ is defined as $\frac{\partial log X(t)}{\partial log a} = \frac{a}{X(t,a)}X_a(t, a)$, and it indicates the expected percentage change by doubling the parameter (i.e., a 100% change). It can be seen that doubling the value of $\alpha$ decreases the healthy tree density by 0.39%, increases the infected tree density by 2.67% and corresponds to a slight increase in the RSW growth rate in 10 days. On doubling the parameter $q$, there are slight changes in the species population. The effect of doubling the parameter $\zeta$ increases the healthy tree density by 0.01%, decreases the infected tree density by 0.098% and corresponds to an RSW population decrease of 5.9%. Hence, comparatively, the spread of the disease is mainly due to the contact rate $\alpha$.

## 5. Optimal control problem

We implemented this task with an aim to minimize the cost due to insecticide spraying. An optimal control problem was formulated with the control $\delta(t)$. It is assumed that insecticide spraying covers all of the pest population in a particular area. The reformulated model with the control $0 \leq \delta(t) \leq 1$ is given by

$$\frac{dH}{dt} = rH\left(1 - \frac{H+I}{k}\right) - (1-\delta)\alpha HW, \tag{5.1}$$

$$\frac{dI}{dt} = (1-\delta)\alpha HW - pI, \tag{5.2}$$

$$\frac{dW}{dt} = (1-\delta)qI - \zeta W, \tag{5.3}$$

with the following initial conditions:

$$H(0) = H_0, \;\; I(0) = I_0, \;\; W(0) = W_0. \tag{5.4}$$

We assume that $H_0 > 0, \; I_0 > 0$ and $W_0 > 0$. The control term $\delta$ denotes the reduction in the infection rate due to the effect of insecticide. The cost function incorporating the existence of optimal spraying is considered in quadratic form, as follows:

$$J(\delta(t)) = \int_{t_0}^{t_f} \left(RI + P\delta(t)^2\right) dt. \tag{5.5}$$

Here $R$ and $P$ are positive constants. The objective functional is chosen so that the first term represents crop damage in infected trees and the cost associated with spraying insecticide is represented in the second term. Our aim was to find an optimal $\delta(t)$ for the minimum cost.

The Hamiltonian $\Psi$ to solve the optimal control problem is constructed as follows:

$$\begin{aligned}\Psi = RI + P\delta(t)^2 + \phi_1\left[rH\left(1 - \frac{H+I}{k}\right) - (1-\delta)\alpha HW\right] \\ +\phi_2\left[(1-\delta)\alpha HW - pI\right] + \phi_3\left[(1-\delta)qI - \zeta W\right],\end{aligned} \tag{5.6}$$

where $\phi_i, \; i = 1, 2, 3$ represents the adjoint variables. For the existence of optimal control, we apply the Pontryagin minimum principle and obtain the result, as follows:

**Theorem 1.** If the objective function $J(\delta)$ is minimized for the optimal control $\delta^*(t)$, then there exists adjoint variables $\phi_i, \; i = 1, 2, 3$, that satisfy the equations below:

$$\frac{d\phi_1}{dt} = -\phi_1 r + \phi_1 r\left(\frac{2H+I}{k}\right) - \alpha W(1-\delta)(\phi_2 - \phi_1), \tag{5.7}$$

$$\frac{d\phi_2}{dt} = -R + \phi_1 r\left(\frac{H}{k}\right) + \phi_2 p - \phi_3(1-\delta)q, \tag{5.8}$$

$$\frac{d\phi_3}{dt} = (1-\delta)\alpha H(\phi_1 - \phi_2) + \phi_3\zeta, \tag{5.9}$$

with the transversality condition satisfying $\phi_i(t_f) = 0,\ i = 1, 2, 3$. The optimal control policy is given by

$$\delta^*(t) = max\left\{0, min\left\{1, \frac{\alpha HW(\phi_2 - \phi_1) + \phi_3 qI}{2P}\right\}\right\}. \tag{5.10}$$

*Proof.* If we apply the Pontryagin minimum principle [19], the optimal control variable $\delta^* \in (0, 1)$ satisfies

$$\frac{\partial \Psi}{\partial \delta^*} = 0. \tag{5.11}$$

From Eqs (5.6) and (5.11), we get

$$\delta^* = \frac{\alpha HW(\phi_2 - \phi_1) + \phi_3 qI}{2P}. \tag{5.12}$$

The boundedness of optimal control takes the form

$$\delta^* = \begin{cases} 0, & \frac{\alpha HW(\phi_2 - \phi_1) + \phi_3 qI}{2P} \leq 0, \\ \frac{\alpha HW(\phi_2 - \phi_1) + \phi_3 qI}{2P}, & 0 < \frac{\alpha HW(\phi_2 - \phi_1) + \phi_3 qI}{2P} < 1, \\ 1, & \frac{\alpha HW(\phi_2 - \phi_1) + \phi_3 qI}{2P} \geq 1. \end{cases} \tag{5.13}$$

Hence, the compact form of $\delta^*$ is given by Eq (5.10). The above equations are the necessary conditions satisfying the optimal control $\delta$ and the state variables of the system. According to [19], the existence conditions are established by the corresponding adjoint equations:

$$\frac{d\phi_1}{dt} = -\frac{\partial \Psi}{\partial H}, \ \frac{d\phi_2}{dt} = -\frac{\partial \Psi}{\partial I}, \ \frac{d\phi_3}{dt} = -\frac{\partial \Psi}{\partial W}. \tag{5.14}$$

From the set of equations in Eq (5.14), we get Eqs (5.7)–(5.9).

## 6. Approximate analytical solution

Liao [25, 26] proposed a powerful analytical method for solving nonlinear problems, called the HAM, to obtain a series of solutions. The basic idea of the HAM is to produce a succession of approximate solutions that tend to the exact solution of the problem. Since the auxiliary parameter $\hbar$ is present in the approximate solution, a family of approximate solutions is produced rather than a single solution, as with standard perturbation methods. The range and rate of convergence of the solution series can be adjusted by changing this auxiliary parameter.

To construct the HAM solution for the model, we denote

$$H(0) = H_0(t) = H_0, \tag{6.1}$$

$$I(0) = I_0(t) = I_0, \tag{6.2}$$

$$W(0) = W_0(t) = W_0. \tag{6.3}$$

The auxiliary linear operators $L_1, L_2$ and $L_3$ with the embedding parameter $\rho \in [0, 1]$ are chosen as

$$L_1[H(t, \rho)] = \frac{dH(t, \rho)}{dt}, \tag{6.4}$$

$$L_2[I(t,\rho)] = \frac{dI(t,\rho)}{dt}, \tag{6.5}$$

$$L_3[W(t,\rho)] = \frac{dW(t,\rho)}{dt}. \tag{6.6}$$

The constant values $L_j(A_j) = 0$, where $A_j(j = 1, 2, 3)$ are integral constants. Define the nonlinear operators as follows:

$$N_1[H, I, W] = \dot{H} - rH\left[1 - \frac{H + I}{k}\right] + \alpha HW, \tag{6.7}$$

$$N_2[H, I, W] = \dot{I} - \alpha HW + pI, \tag{6.8}$$

$$N_3[H, I, W] = \dot{W} - qI + \zeta W. \tag{6.9}$$

The zero-order deformation equations, according to Liao, can be defined as

$$(1 - \rho)L_1[H(t;\rho) - H_0(t)] = \rho\hbar_1 H_1(t)N_1[H, I, W], \tag{6.10}$$

$$(1 - \rho)L_2[I(t;\rho) - I_0(t)] = \rho\hbar_2 H_2(t)N_2[H, I, W], \tag{6.11}$$

$$(1 - \rho)L_3[W(t;\rho) - W_0(t)] = \rho\hbar_3 H_3(t)N_3[H, I, W], \tag{6.12}$$

where $\rho \in [0, 1]$ is the embedding parameter, $\hbar \neq 0$ is a nonzero auxiliary parameter, $H(t) \neq 0$ is an auxiliary function and $L$ is an auxiliary linear operator. It is essential to note that, with the HAM, one has a considerable deal of flexibility in selecting auxiliary unknowns.

When $\rho = 0$ and $\rho = 1$, it follows that

$$H(t;0) = H_0(t) \text{ and } H(t;1) = H(t), \tag{6.13}$$

$$I(t;0) = I_0(t) \text{ and } I(t;1) = I(t), \tag{6.14}$$

$$W(t;0) = W_0(t) \text{ and } W(t;1) = W(t). \tag{6.15}$$

As $\rho$ tends to rise from 0 to 1, the terms $H(t;\rho)$, $I(t;\rho)$ and $W(t;\rho)$ change from the initial guess to the final solution. With regard to $\rho$, we can expand these terms in a Taylor series as follows:

$$H(t;\rho) = H_0(t) + \sum_{m=1}^{\infty} H_m(t)\rho^m, \tag{6.16}$$

$$I(t;\rho) = I_0(t) + \sum_{m=1}^{\infty} I_m(t)\rho^m, \tag{6.17}$$

$$W(t;\rho) = W_0(t) + \sum_{m=1}^{\infty} W_m(t)\rho^m, \tag{6.18}$$

where

$$H_m = \frac{1}{m!}\frac{\partial^m H(t;\rho)}{\partial\rho^m}\bigg|_{\rho=0}, \tag{6.19}$$

$$I_m = \frac{1}{m!}\frac{\partial^m I(t;\rho)}{\partial\rho^m}\bigg|_{\rho=0}, \tag{6.20}$$

$$W_m = \frac{1}{m!}\frac{\partial^m W(t;\rho)}{\partial \rho^m}\bigg|_{\rho=0}. \tag{6.21}$$

The series converges at $\rho = 1$ if the auxiliary linear operator, the initial guess, the auxiliary parameter and the auxiliary function are all chosen suitably. Then, we have

$$H(t) = H_0(t) + \sum_{m=1}^{\infty} H_m(t), \tag{6.22}$$

$$I(t) = I_0(t) + \sum_{m=1}^{\infty} I_m(t), \tag{6.23}$$

$$W(t) = W_0(t) + \sum_{m=1}^{\infty} W_m(t). \tag{6.24}$$

We can obtain the so-called $m^{th}$-order deformation equation by differentiating Eqs (6.10)–(6.12) $m$ times with regard to the embedding parameter $\rho$, then setting $\rho = 0$ and dividing them by $m!$.

$$L_1[H_m(t) - \Omega_m H_{m-1}(t)] = \hbar M_{1,m}(H_{m-1}(t)), \tag{6.25}$$

$$L_2[I_m(t) - \Omega_m I_{m-1}(t)] = \hbar M_{2,m}(I_{m-1}(t)), \tag{6.26}$$

$$L_3[W_m(t) - \Omega_m W_{m-1}(t)] = \hbar M_{3,m}(W_{m-1}(t)), \tag{6.27}$$

where

$$M_{1,m}(t) = \frac{dH_{m-1}(t)}{dt} - rH_{m-1} + \frac{r}{k}\sum_{s=0}^{m-1} H_s(t)H_{m-1-s}(t) + \frac{r}{k}\sum_{s=0}^{m-1} H_s(t)I_{m-1-s}(t) + \alpha\sum_{s=0}^{m-1} H_s(t)W_{m-1-s}(t), \tag{6.28}$$

$$M_{2,m}(t) = \frac{dI_{m-1}(t)}{dt} - \alpha\sum_{s=0}^{m-1} H_s(t)W_{m-1-s}(t) + pI_{m-1}(t), \tag{6.29}$$

$$M_{3,m}(t) = \frac{dW_{m-1}(t)}{dt} - qI_{m-1-s}(t) + \zeta W_{m-1}(t), \tag{6.30}$$

and

$$\Omega_m = \begin{cases} 0, & m \le 1 \\ 1, & m > 1 \end{cases}.$$

For $m \ge 1$, the $m^{th}$- order deformation equation becomes

$$H_m(t) = \Omega_m H_{m-1}(t) + \hbar\int_0^t M_{1,m}(\tau)d\tau, \tag{6.31}$$

$$I_m(t) = \Omega_m I_{m-1}(t) + \hbar\int_0^t M_{2,m}(\tau)d\tau, \tag{6.32}$$

$$P_m(t) = \Omega_m W_{m-1}(t) + \hbar\int_0^t M_{3,m}(\tau)d\tau. \tag{6.33}$$

In this way, we may easily derive $H_m$, $I_m$ and $W_m$ for $m \geq 1$ at the $M^{th}$ order. Then, we have

$$H(t) = \sum_{m=0}^{M} H_m(t),\ I(t) = \sum_{m=0}^{M} I_m(t) \text{ and } W(t) = \sum_{m=0}^{M} W_m(t). \tag{6.34}$$

The approximate analytical solution of the system is given by

$$\begin{aligned} H(t) = H_0 + \frac{t}{k}\Big[(r+\hbar)(H_0+I_0) + H_0^2 r\hbar + H_0 I_0 r\hbar - 2\hbar H_0 kr + 2W_0 H_0 k\alpha\hbar + W_0 H_0 k\hbar^2 \\ -rH_0 h\hbar^2\Big] + \frac{H_0^2\hbar^2 t^2}{2k^2}\Big[r^2k^2 - 2W_0k^2\alpha r + H_0^2\alpha^2k^2 - I_0q\alpha k^2 + \zeta W_0\alpha k^2 + 2W_0k\alpha r(H_0+I_0) \\ +I_0prk + 3H_0r^2(I_0-k) + 2H_0^2r^2 - r^2\Big], \end{aligned} \tag{6.35}$$

$$\begin{aligned} I(t) = I_0 + t\Big[2I_0p\hbar - 2\alpha\hbar H_0W_0 + \hbar^2(I_0p - \alpha H_0W_0)\Big] + \frac{H_0\hbar^2t^2}{k}\Big[I_0p^2 - I_0\alpha W_0r - W_0^2H_0r\alpha \\ -kW_0^2\alpha^2 - k\alpha W_0p - k\zeta\alpha W_0 + kr\alpha W_0 + kI_0q\alpha\Big], \end{aligned} \tag{6.36}$$

$$W(t) = W_0 + t\Big[2\hbar\zeta W_0 - 2\hbar I_0q - I_0q\hbar^2 - \zeta W_0\hbar^2\Big] + \frac{t^2\hbar^2}{2}\Big[H_0W_0\alpha q + \zeta^2W_0 - I_0q(p+\zeta)\Big]. \tag{6.37}$$

This is the solution for $M = 2$. We calculated up to the sixth-order solution using Maple. Since we obtain a more approximate solution for the sixth order, we stopped at this iteration. Similarly, we can find higher-order solutions until the solution converges [27–30]. It is important to note that the auxiliary parameter $\hbar$ plays a key role in the solution series convergence and accuracy. The approximate solution given by Eqs (6.35)–(6.37) contains $\hbar$. A multiple of $\hbar$ - curves were plotted to define a region such that the solution series is independent of $\hbar$. The convergence region for the corresponding solution is the region where the distributions of $H$ and $H'$ versus $\hbar$ are horizontal lines. The overall convergence region is the common region between the variable and its derivatives. Such $\hbar$ - curves are plotted in Figures 4–6. These figures clearly show that the appropriate range of $\hbar$ is about $-1.1 \leq \hbar \leq -0.9$.

## 7. Results and discussion

To carry out the numerical analysis, we selected values that would provide a reference point for each parameter. Each coconut tree occupies an area ranging from 7.5 m × 7.5 m to 8.5 m × 8.5 m. We consider this in terms of density per square meter and the initial conditions are assumed to be $H(0) = 0.005\text{m}^{-2}$ and $I(0) = 0.0007\text{m}^{-2}$. We assume the whitefly population approximately as $W(0) = 2\text{m}^{-2}$. The parameter values were framed based on the facts and methods in [8]. The carrying capacity was calculated as density per square meter of a tree. The whitefly population is relevant as in the case of ACMD given in [8]; hence, we use those values. The replanting rate and mortality rate are assumed to be one tree in 120 days. The contact rate between RSWs and coconut trees were calculated as the number of trees infected in adult emergence per RSW, i.e., 0.5–1 tree in 25 days [8]. Table 1 comprises all of the parameter values. The numerical simulations were carried out using MATLAB. Figure 1 interprets that the contact rate $\alpha$ decreases the healthy tree density. The replanting rate $r$

and whitefly death rate $\zeta$ increases the healthy tree density. From Figure 2, we see that the contact rate $\alpha$ increases the infected tree density. $\zeta$ and $p$ decrease the infected tree density as expected. Figure 3 shows the decrease in whitefly population according to its death rate. Figure 4 represents the $\hbar$ curve of the sixth-order solution of $H(t)$ at $t = 1$, where the horizontal line denotes the convergence region. Figures 5 and 6 represents the $\hbar$ curve of the sixth-order solutions of $I(t)$ and $W(t)$ at $t = 1$, respectively. The $\hbar$ -curves clearly show that the appropriate range of $\hbar$ is about $-1.1 \leq \hbar \leq -0.9$. Thus, the maximum error obtained by comparing the analytical and numerical results does not exceed 0.4% for all possible values of parameters. In Figures 7 and 8, we portray the sensitivity analysis with the parameters $\alpha$, $q$ and $\zeta$ in the proposed model. It is observed that, due to the contact rate $\alpha$, the tree density is affected at a higher rate compared to other parameters.

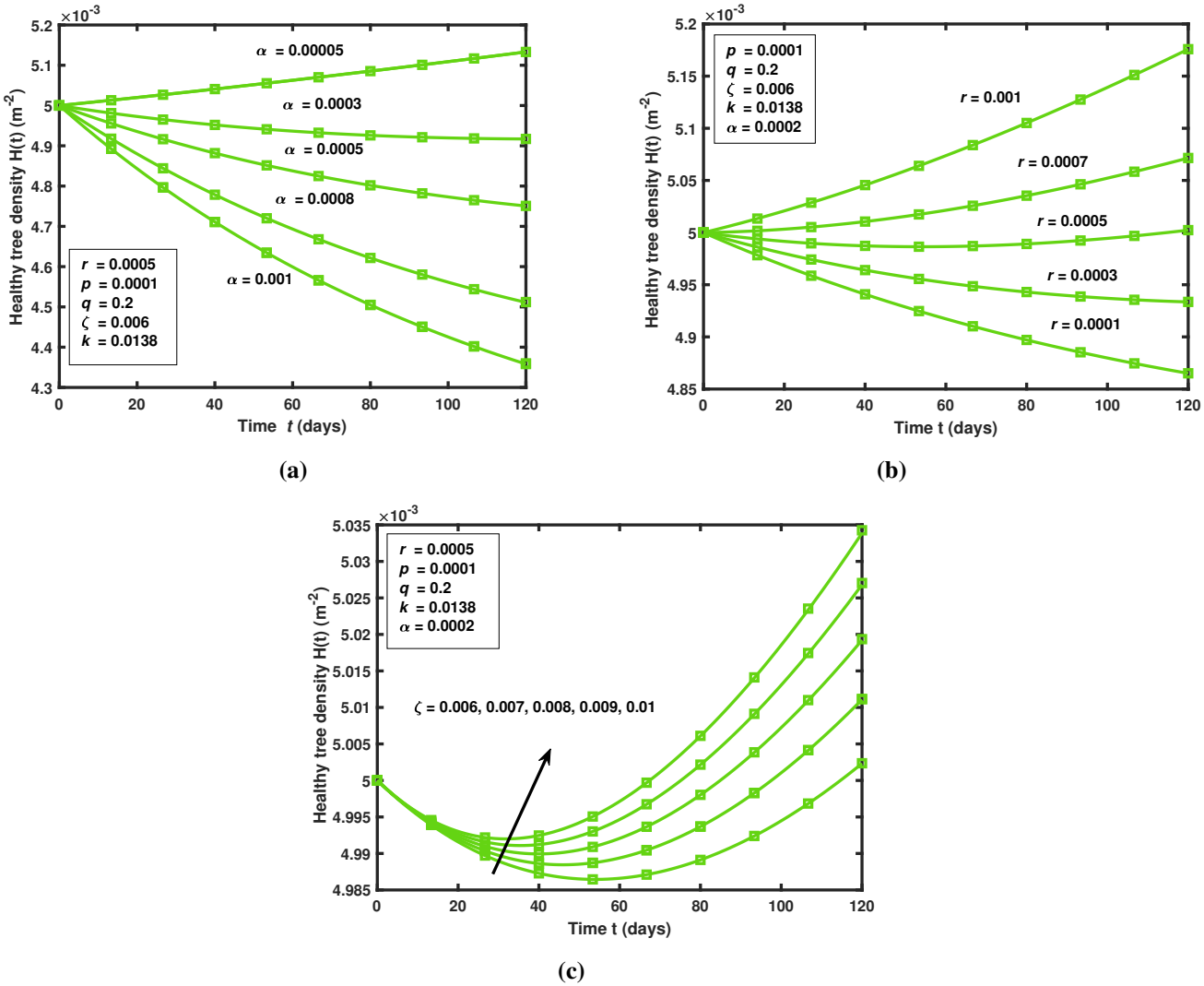


**Figure 1.** Profiles of healthy tree density $H$ versus time $t$, obtained by applying the HAM solution and numerical simulations. The curves denoted by ▫ represent the HAM solution (Eq (6.35)), and — represents the numerical simulation.

**Table 1.** Parameter values used for analysis, as calculated based on [8].

| Symbol | Meaning | Unit | Value taken for analysis | Range |
|---|---|---|---|---|
| $k$ | Tree density | $m^{-2}$ | 0.0138 | 0.0138 – 0.0178 |
| $r$ | Replanting rate | $day^{-1}$ | 0.0005 | 0 – 0.008 |
| $p$ | Mortality rate for trees | $day^{-1}$ | 0.0002 | 0 – 0.008 |
| $\alpha$ | Contact rate | $pest^{-1}day^{-1}$ | 0.0002 | 0 – 0.002 |
| $q$ | Whitefly birth rate | $day^{-1}$ | 0.1 | 0.1 – 0.3 |
| $\zeta$ | Death rate for RSWs | $day^{-1}$ | 0.006 | 0.006 – 0.01 |

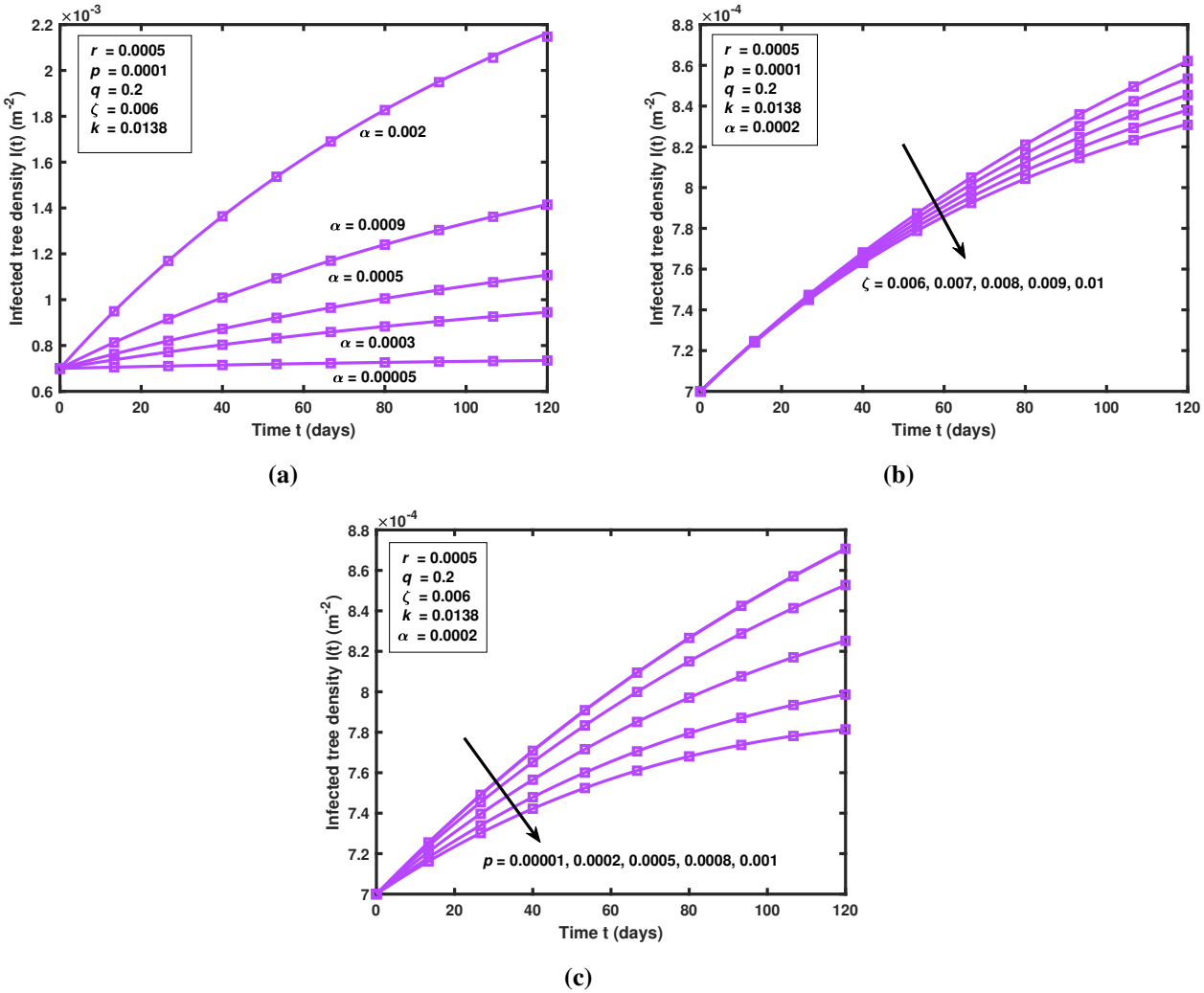


**Figure 2.** Profiles of infected tree density $I$ versus time $t$, obtained by applying the HAM solution and numerical simulations. The curves denoted by ▫ represent the HAM solution (Eq (6.36)), and —— represents the numerical simulation.

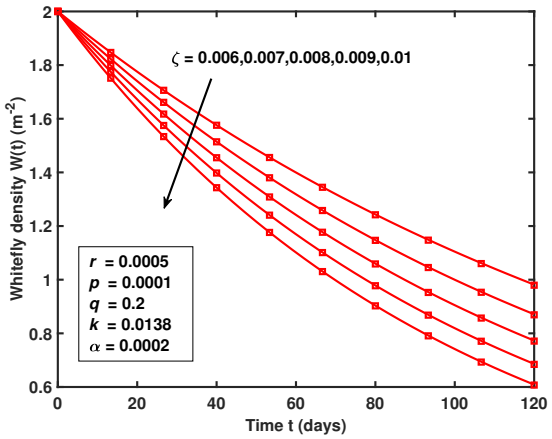


**Figure 3.** Profiles of whitefly density $W$ versus time $t$, obtained by applying the HAM solution and numerical simulations. The curves denoted by ◻ represent the HAM solution (Eq (6.37)), and — represents numerical simulations.

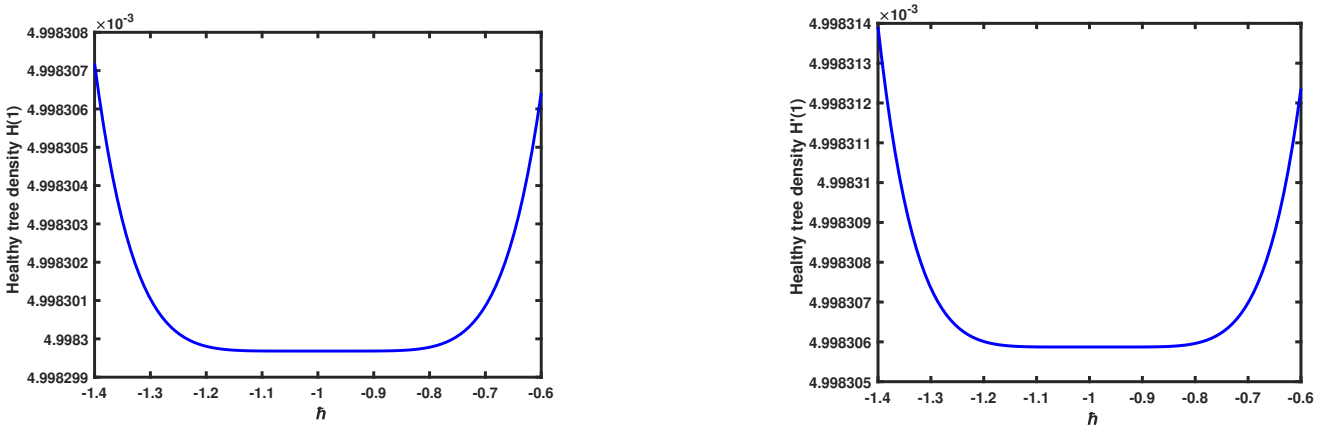


**(a)** **(b)**

**Figure 4.** $\hbar$ curves for the sixth-order solutions of (a) $H(t)$ and (b) $H'(t)$ at $t = 1$.

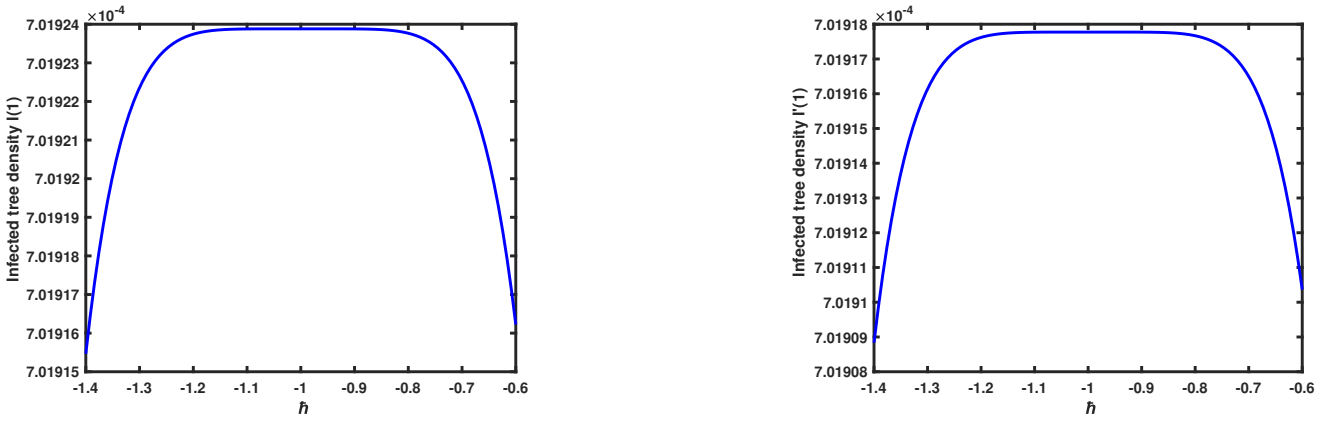


**(a)** **(b)**

**Figure 5.** $\hbar$ curves for the sixth-order solutions of (a) $I(t)$ and (b) $I'(t)$ at $t = 1$.

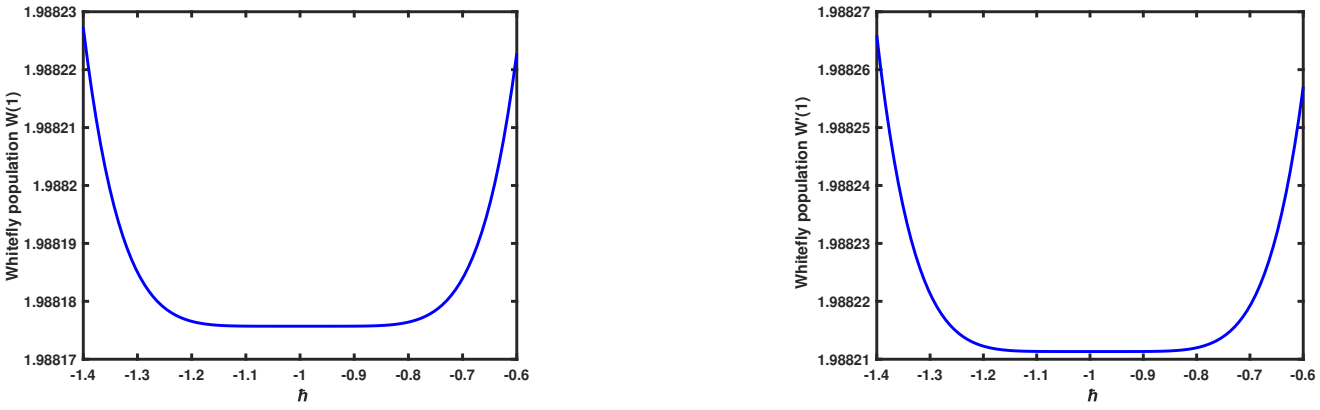


(a) (b)

**Figure 6.** $\hbar$ curves for the sixth-order solutions of (a) $W(t)$ and (b) $W'(t)$ at $t = 1$.

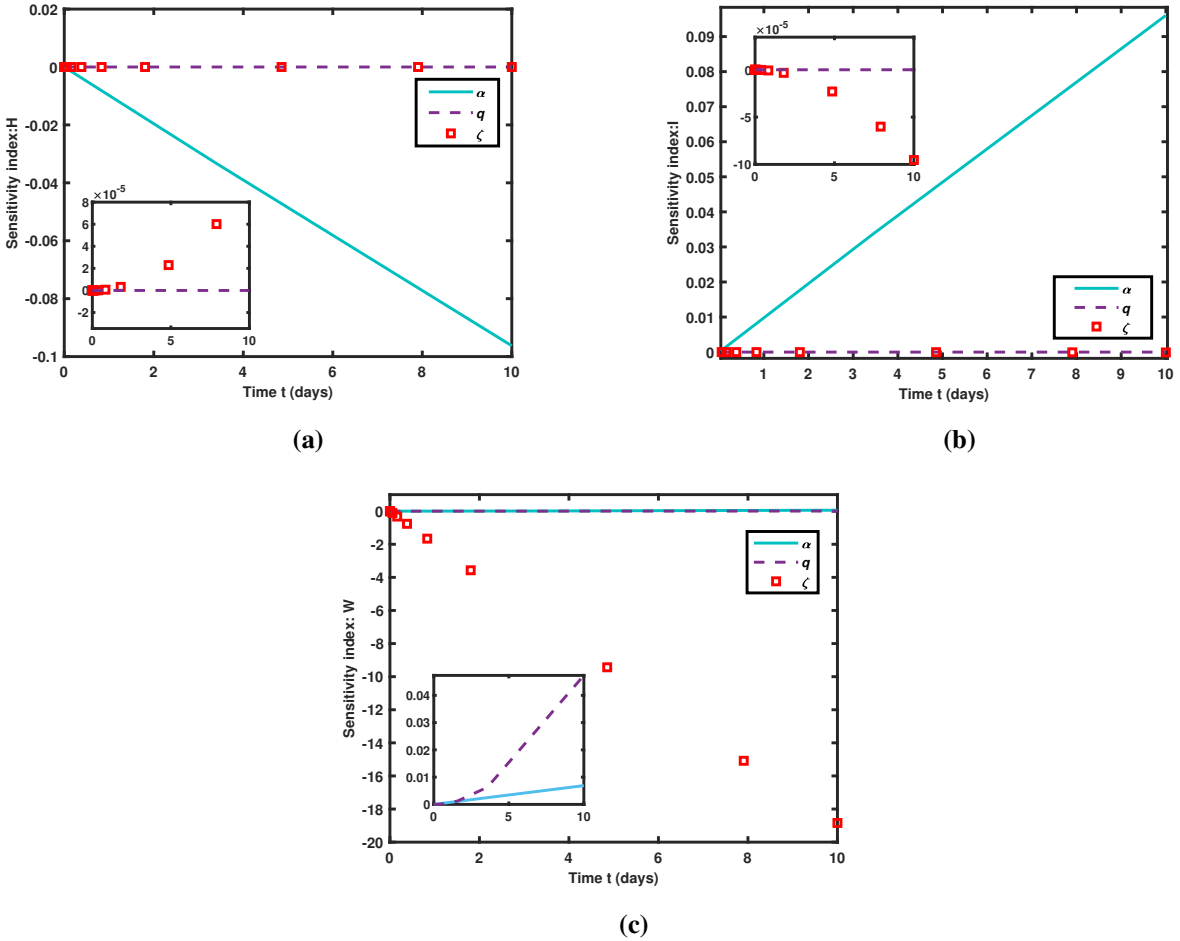


(a) (b)

(c)

**Figure 7.** Sensitivity index for the species parameters $\alpha$, $q$ and $\zeta$. This figure denotes the partial derivative of the interacting population with respect to each sensitivity parameters. The parameter values used for analysis are $k = 0.0138$, $r = 0.0005$, $p = 0.0002$, $\alpha = 0.0002$, $q = 0.1$ and $\zeta = 0.006$.

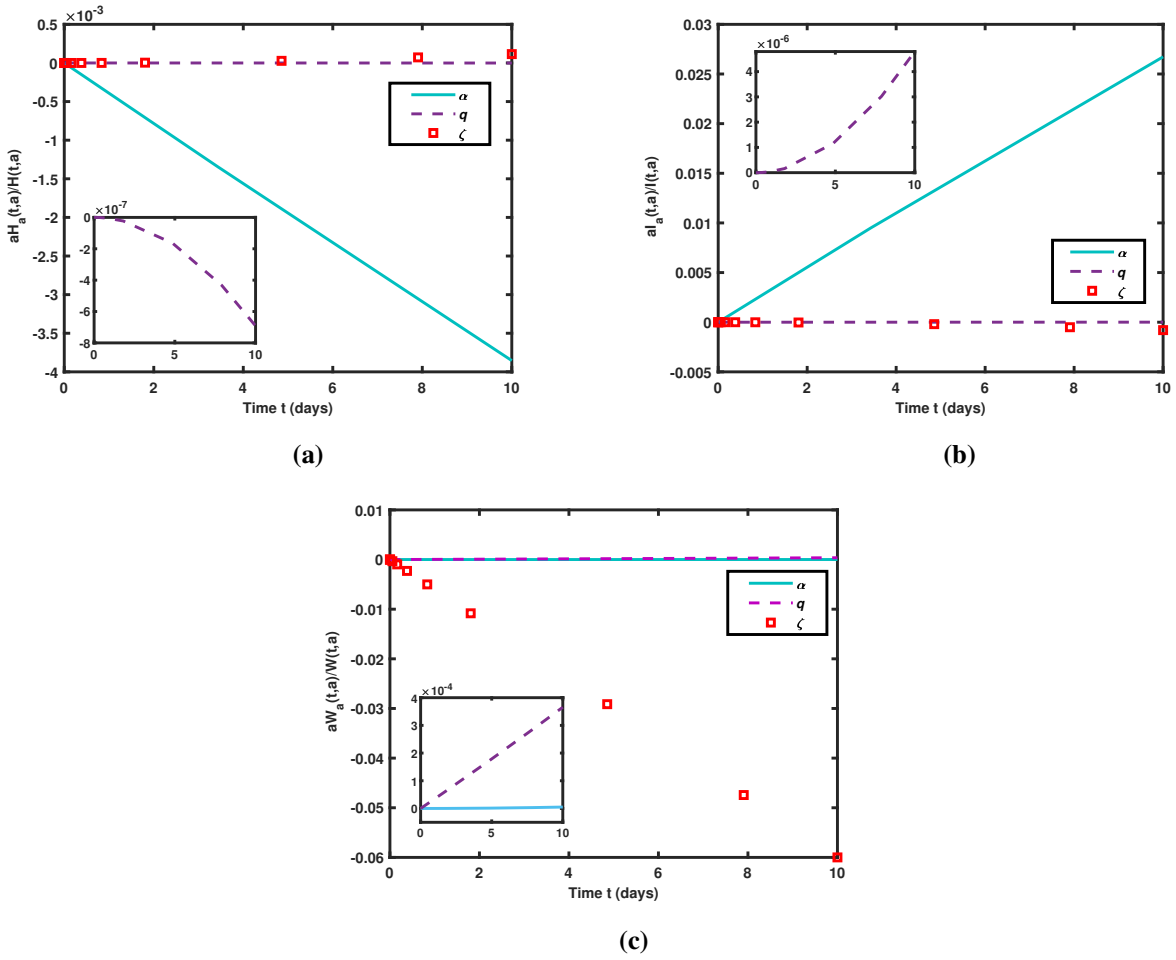


**(a)** **(b)** **(c)**

**Figure 8.** Logarithmic sensitivity analysis in the direction of indicated parameters versus time. Here, $a$ is used as a common term to denote the selected parameters. The parameter values used for analysis are $k = 0.0138$, $r = 0.0005$, $p = 0.0002$, $\alpha = 0.0002$, $q = 0.1$ and $\zeta = 0.006$.

Figure 9 indicates the population dynamics of our model with and without the optimal control effect. The initial conditions for the optimal control problem were set as $H_0 = 20$, $I_0 = 5$ and $W_0 = 10$. Based on the initial conditions, the value of the tree density $k$ was set to be 70. The main reason for using the control term is to reduce the infected tree density so that its growth and yield are not affected. It can be seen that there are measurable differences between the models with and without the control effect for the healthy trees, infected trees and whitefly population. Figure 10 denotes the control effect $\delta(t)$ versus time. The control can be achieved by insecticide spraying. Thus, optimal spraying is needed to control the spread of the disease.

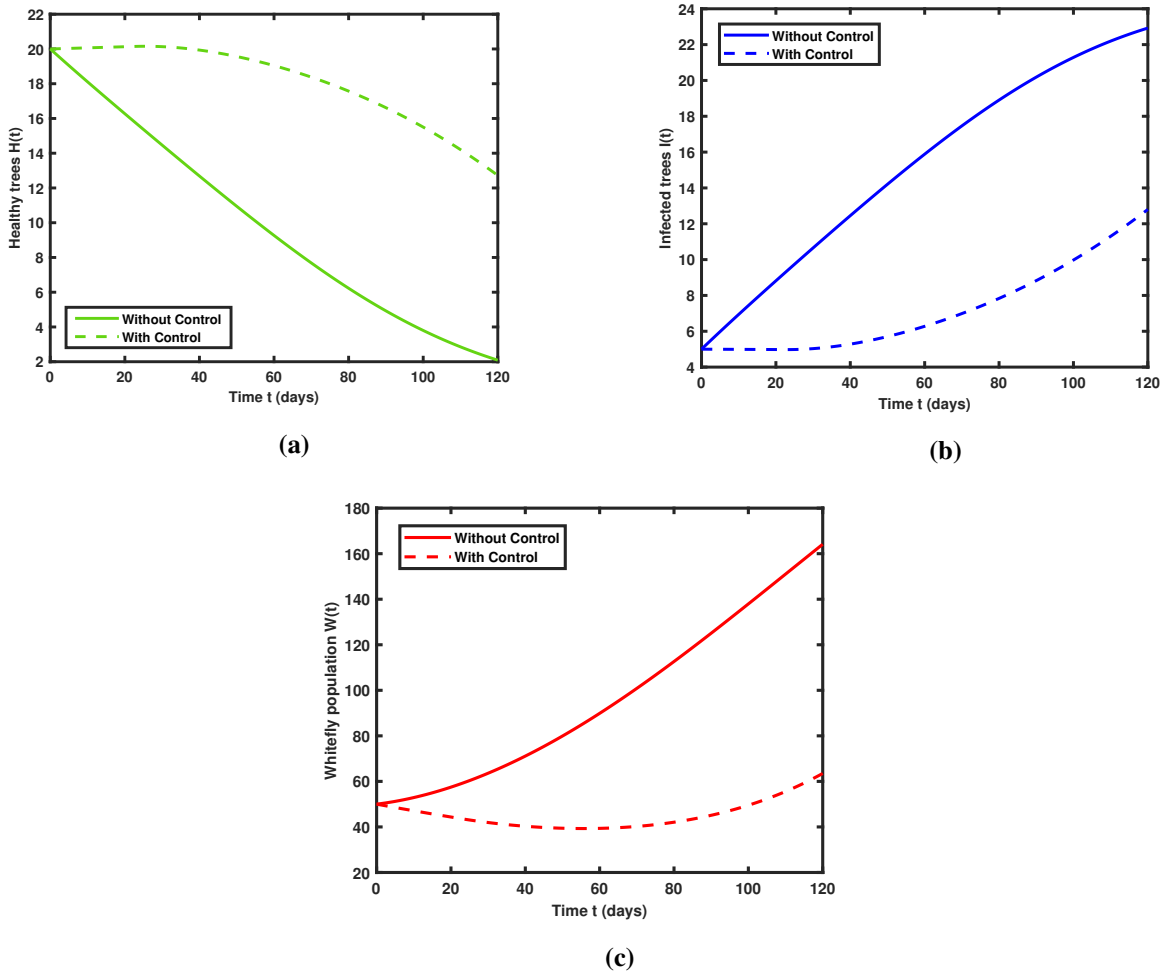


**Figure 9.** Comparison of the population densities of the system given by Eqs (2.1)–(2.3) with the system given by Eqs (5.1)–(5.3). The values for the initial conditions and parameters used for the analysis are $H(0) = 20$, $I(0) = 5$, $W(0) = 50$, $k = 70$, $r = 0.0005$, $p = 0.0002$, $\alpha = 0.0002$, $q = 0.1$ and $\zeta = 0.006$. The use of control increases the healthy tree density and reduces the infection.

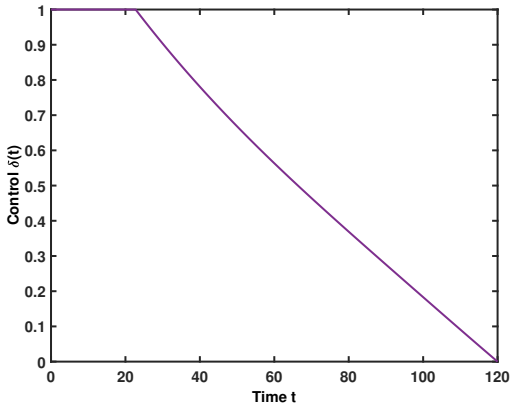


**Figure 10.** Plot of the control function $\delta(t)$ versus time, with the parameter values given in Table 1.

## 8. Conclusions

In this paper, the impact of the dynamics of interacting species' population and parameters on the system were analyzed. We focused on the interaction between RSWs and coconut trees within a locality. The equilibrium points and the conditions to be LAS and GAS have been analyzed. A sensitivity analysis was carried out to observe the system dynamics and the state variables in the direction of selected parameters. An optimal control model has been proposed and analyzed using the Pontryagin minimum principle. An approximate analytical solution has been derived using the HAM. To validate the convergence region, $\hbar$-curves were derived. From the comparison of the numerical simulation results and analytical results, we found good agreement between them. From the above study, it is strongly indicated that the contact rate $\alpha$ stands as a crucial determining factor. Thus, by decreasing the contact rate with the effective usage of control measures can help the farmers, in a great way, to control the disease.

## Acknowledgement

The authors are very thankful to the management at the SRM Institute of Science and Technology for their continuous support and encouragement.

## Conflict of interest

The authors declare there is no conflict of interest.

## References

1. K. Elango, S. J. Nelson, A. Aravind, Rugose spiralling whitefly, Aleurodicus rugioperculatus Martin (Hemiptera, Aleyrodidae): An invasive foes of coconut, *J. Entomol. Res.*, **44** (2020), 261–266. http://dx.doi.org/10.5958/0974-4576.2020.00046.8
2. S. Shanas, J. Job, T. Joseph, G. Anju Krishnan, First report of the invasive rugose spiraling whitefly, Aleurodicus rugioperculatus Martin (Hemiptera: Aleyrodidae) from the old world, *Entomon*, **41** (2016), 365–368. Available from: https://www.entomon.in/index.php/Entomon/article/view/227.
3. T. Srinivasan, P. A. Saravanan, A. Josephrajkumar, K. Rajamanickam, S. Sridharan, P. M. M. David, et al., Invasion of the rugose spiralling whitefly, Aleurodicus rugioperculatus Martin (Hemiptera: Aleyrodidae) in Pollachi tract of Tamil Nadu, India, *Madras Agric. J.*, **103** (2016), 349–353. Available from: http://masujournal.org/index.php.
4. R. Sundararaj, K. Selvaraj, Invasion of rugose spiraling whitefly, Aleurodicus rugioperculatus Martin (Hemiptera: Aleyrodidae): A potential threat to coconut in India, *Phytoparasitica*, **45** (2017), 71–74. http://dx.doi.org/10.1007/s12600-017-0567-0
5. M. Visalakshi, K. Selvaraj, B. P. B. Sumalatha, Biological control of invasive pest, rugose spirallying whitefly in coconut and impact on environment, *J. Entomol. Zool. Stud.*, **9** (2021), 1215–1218. https://dx.doi.org/10.22271/j.ento

6. K. Elango, S. J. Nelson, S. Sridharan, V. Paranidharan, S. Balakrishnan, Biology, distribution and host range of new invasive pest of India coconut rugose spiralling whitefly Aleurodicus rugioperculatus Martin in Tamil Nadu and the status of its natural enemies, *Int. J. Agricul. Sci.*, **11** (2019), 8423–8426. Available from: http://www.bioinfopublication.org/pages/journal.php?id=BPJ0000217.
7. L. J. Allen, F. Brauer, P. Van den Driessche, J. Wu, *Mathematical epidemiology*, Springer, Berlin, 2019.
8. J. Holt, M. J. Jeger, J. M. Thresh, G. W. Otim-Nape, An epidemilogical model incorporating vector population dynamics applied to African cassava mosaic virus disease, *J. Appl. Ecol.*, **34** (1997), 793–806. https://doi.org/10.2307/2404924
9. S. Ray, F. A. Basir, Impact of incubation delay in plant-vector interaction, *Math. Comput. Simul.*, **170** (2020), 16–31. https://doi.org/10.1016/j.matcom.2019.09.001
10. F. A. Basir, A. Banerjee, S. Ray, Role of farming awareness in crop pest management-A mathematical model, *J. Theor. Biol.*, **461** (2019), 59–67. https://doi.org/10.1016/j.jtbi.2018.10.043
11. F. A. Basir, P. K. Roy, Dynamics of mosaic disease with roguing and delay in Jatropha curcas plantations, *J. Appl. Math. Comput.*, **58** (2018), 1–31. https://doi.org/10.1007/s12190-017-1131-2
12. E. Venturino, P. K. Roy, F. A. Basir, A. Datta, A model for the control of the mosaic virus disease in Jatropha curcas plantations, *Energy Ecol. Environ.*, **1** (2016), 360–369. http://dx.doi.org/10.1007/s40974-016-0033-8
13. S. Wang, Z. Ma, X. Li, T. Qi, A generalized delay-induced SIRS epidemic model with relapse, *AIMS Math.*, **7** (2022) 6600–6618. http://dx.doi.org/10.3934/math.2022368
14. R. ud Din, K. Shah, M. A. Alqudah, T. Abdeljawad, F. Jarad, Mathematical study of SIR epidemic model under convex incidence rate, *AIMS Math.*, **5** (2020), 7548–7561. http://dx.doi.org/10.3934/math.2020483
15. P. Van den Driessche, J. Watmough, Reproduction numbers and sub-threshold endemic equilibria for compartmental models of disease transmission, *Math. Biosci.*, **180** (2002), 29–48. https://doi.org/10.1016/S0025-5564(02)00108-6
16. J. P. LaSalle, *The stability of dynamical systems*, Regional Conference Series in Applied Mathematics, SIAM, Philadelphia, 1976.
17. D. M. Bortz, P. W. Nelson, Sensitivity analysis of a nonlinear lumped parameter model of HIV infection dynamics, *Bull. Math. Biol.*, **66** (2004), 1009–1026. http://dx.doi.org/10.1016/j.bulm.2003.10.011
18. A. K. Misra, M. Verma, Modeling the impact of mitigation options on abatement of methane emission from livestock, *Nonlinear Anal.-Model.*, **22** (2017), 210–229. https://doi.org/10.15388/NA.2017.2.5
19. L. S. Pontryagin, V. G. Boltyanskii, R. V. Gamkrelidze, E. F. Mishchenko, *Mathematical theory of optimal processes*, Inderscience, New York, 1962.
20. S. Lenhart, J. T. Workman, *Optimal control applied to biological models*, CRC Press, New York, 2007.
21. X. Wang, *Solving optimal control problems with MATLAB: Indirect methods*, Technical report ISE. Dept., NCSU, 2009.
22. T. Vijayalakshmi, R. Senthamarai, An analytical approach to the density dependent prey-predator system with Beddington-Deangelies functional response, *AIP Conf. Proc.*, **2112** (2019), 020077. https://doi.org/10.1063/1.5112262

23. R. Senthamarai, L. Rajendran, System of coupled non-linear reaction diffusion processes at conducting polymer-modified ultramicroelectrodes, *Electrochimica Acta*, **55** (2010), 3223–3235. https://doi.org/10.1016/j.electacta.2010.01.013
24. M. Abbasi, D. D. Ganji, I. Rahimipetroudi, M. Khaki, Comparative analysis of MHD boundary-layer flow of viscoelastic fluid in permeable channel with slip boundaries by using HAM, VIM, HPM, *Walailak J. Sci. Technol.*, **11** (2014), 551–567. Available from: `https://103.58.148.28/index.php/wjst/article/view/619`.
25. S. Liao, *Beyond perturbation: Introduction to the homotopy analysis method*, CRC Press, New York, 2003.
26. S. Liao, On the homotopy analysis method for nonlinear problems, *Appl. Math. Comput.*, **147** (2004), 499–513. https://doi.org/10.1016/S0096-3003(02)00790-7
27. S. Noeiaghdam, M. Suleman, H. Budak, Solving a modified nonlinear epidemiological model of computer viruses by homotopy analysis method, *Math. Sci.*, **12** (2018), 211–222 . https://doi.org/10.1007/s40096-018-0261-5
28. P. A. Naik, J. Zu, M. Ghoreishi, Stability analysis and approximate solution of SIR epidemic model with Crowley-Martin type functional response and holling type II treatment rate by using homotopy analysis method, *J. Appl. Anal. Comput.*, **10** (2020), 1482–1515. http://dx.doi.org/10.11948/20190239
29. J. Duarte, C. Januário, N. Martins, C. C. Ramos, C. Rodrigues, J. Sardanyés, Optimal homotopy analysis of a chaotic HIV-1 model incorporating AIDS-related cancer cells, *Numer. Algorithms*, **77** (2018), 261–288. https://doi.org/10.1007/s11075-017-0314-0
30. P. A. Naik, J. Zu, M. Ghoreishi, Estimating the approximate analytical solution of HIV viral dynamic model by using homotopy analysis method, *Chaos Soliton. Fract.*, **131** (2020), 109500. https://doi.org/10.1016/j.chaos.2019.109500
31. P. Kumar, V. S. Erturk, Environmental persistence influences infection dynamics for a butterfly pathogen via new generalised Caputo type fractional derivative, *Chaos Soliton. Fract.*, **144** (2021), 110672. https://doi.org/10.1016/j.chaos.2021.110672
32. P. Kumar, V. S. Erturk, H. Almusawa, Mathematical structure of mosaic disease using microbial biostimulants via Caputo and Atangana-Baleanu derivatives, *Results Phys.*, **24** (2021), 104186. https://doi.org/10.1016/j.rinp.2021.104186
33. P. Kumar, D. Baleanu, V. S. Erturk, M. Inc, V. Govindaraj, A delayed plant disease model with Caputo fractional derivatives, *Adv. Cont. Discrete Model.*, **1** (2022), 1–22. https://doi.org/10.1186/s13662-022-03684-x
34. P. Kumar, V. Suat Ertürk, K. S. Nisar, Fractional dynamics of huanglongbing transmission within a citrus tree, *Math. Method. Appl. Sci.*, **44** (2021), 11404–11424. https://doi.org/10.1002/mma.7499
35. P. Kumar, V. S. Erturk, V. Govindaraj, S. Kumar, A fractional mathematical modeling of protectant and curative fungicide application, *Chaos Soliton. Fract.,* **8** (2022), 100071. https://doi.org/10.1016/j.csfx.2022.100071



AIMS Press